

Filament stretching of carbon nanotube suspensions

Anson W. K. Ma · Francisco Chinesta · Tri Tuladhar ·
Malcolm R. Mackley

Received: 18 June 2007 / Accepted: 18 November 2007 / Published online: 30 January 2008
© Springer-Verlag 2007

Abstract This paper reports the application of a recently developed filament stretching protocol for the study of the extensional rheology of both treated and untreated carbon nanotubes (CNT) suspended within an epoxy resin. It was experimentally observed that filaments formed by treated and untreated CNT suspensions behaved differently after initial stretching. The filament thinning process of the base epoxy was consistent with a simple Newtonian fluid, whilst the filament of treated CNT suspensions also thinned in a Newtonian way but with an enhanced extensional viscosity. Filaments formed with untreated CNT suspensions behaved in a non-uniform way with local fluctuation in filament diameter, and it was not possible to obtain reliable extensional viscosity data. Irregularity of the untreated CNT filaments was consistent with coupled optical images, where spatial variation in CNT aggregate concentration was observed. In the case of treated CNT suspensions, the enhanced extensional viscosity was modelled in terms of the alignment of CNTs in the stretching direction, and the degree of alignment was subsequently estimated using a simple orientation model.

Keywords Carbon nanotubes · Fibre suspension · Elongational flow · Flow alignment

Introduction

Carbon nanotubes (CNTs) are cylinders of rolled graphene sheets having a very high aspect ratio, typically in the order of several hundreds (Iijima 1991). They belong to a relatively new class of nano-fibrous material that can potentially be used for high-performance composites and electronic devices (Ajayan et al. 1994; Saito 1997; Tans et al. 1998; Calvert 1999). Processing of CNTs into macroscopically usable forms, however, normally requires dispersing them in a suspending medium (Hussain et al. 2006). For example, Davis et al. (2004) reported possible fibre spinning for CNT suspensions by first dispersing CNTs in superacids, and more recently, Kordás et al. (2006) proposed that inkjet printing of CNT suspensions could be a promising way for large-scale production of flexible and conductive CNT composite films. For this type of process, it is important to understand the extensional rheology of CNT suspensions; earlier rheological studies, however, mainly focused on the shear or the linear viscoelastic measurements of CNT suspensions (see, for example, Pötschke et al. 2002; Lin-Gibson et al. 2004; Rahatekar et al. 2006). In the case of carbon nanofibres (CNFs), which are analogous to CNTs, Xu et al. (2005) reported that, for untreated CNFs suspended in a glycerol/water solution, the extensional viscosity decreases as the extensional rate increases, and this is possibly due to the breakup of network structure.

This paper investigates the extensional rheology for both chemically treated and untreated CNT suspensions using the technique of filament stretching (see, for example, McKinley and Sridhar 2002). The findings of this paper are of relevance to understanding the flow behaviour and orientation of CNTs in potential processes such as the fibre spinning (Davis et al. 2004), inkjet printing (Kordás et al.

A. W. K. Ma · T. Tuladhar · M. R. Mackley (✉)
Department of Chemical Engineering, University of Cambridge,
New Museums Site, Pembroke Street,
Cambridge CB2 3RA, UK
e-mail: mrm5@cam.ac.uk

F. Chinesta
Laboratoire de Mécanique des Systèmes et des Procédés,
UMR 8106 CNRS-ENSAM-ESEM,
151 Boulevard de l'Hôpital,
75013 Paris, France

2006) and curtain coating (Jäder et al. 2005) of CNT suspensions.

Experiments

Materials and sample preparation

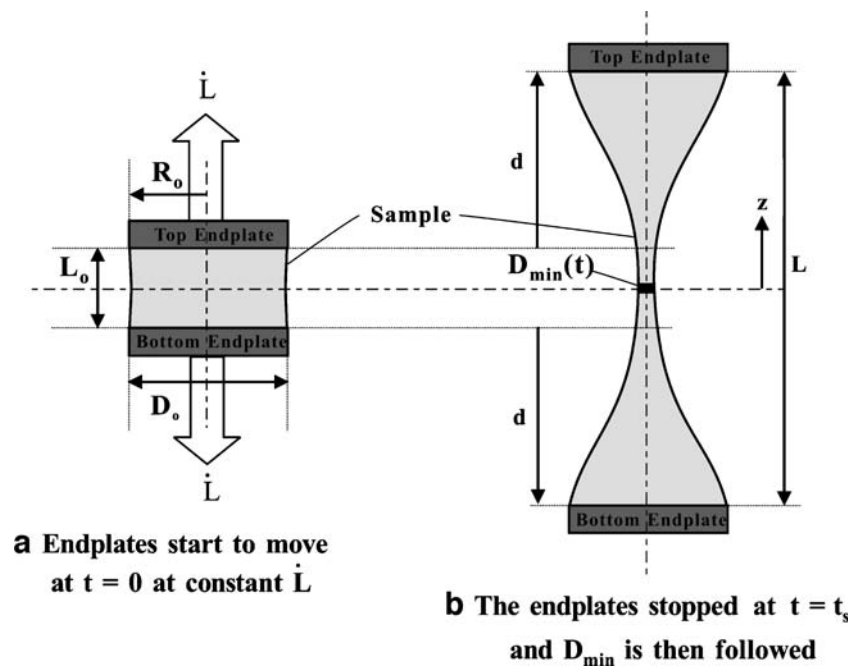
Surface-treated CNTs were single-walled CNTs covalently functionalised with Arene Diazonium salts, and they were provided by Nanocomposites, Houston, TX, USA. Details for the chemical treatment were reported elsewhere (Dyke and Tour 2003, 2004). Small bundles of treated CNTs, with a diameter of about 5 nm and a length of 1 μm , were observed using atomic force microscopy (AFM). Untreated CNTs used were multi-walled and, according to scanning electron microscope (SEM) images, they had a diameter of less than 100 nm. They were produced by the chemical vapour deposition (CVD) method (Singh et al. 2003) at the Department of Materials Science and Metallurgy, University of Cambridge. The exact length of the untreated CNTs was not fully characterised, but optical images suggested that they were bundled and were about 30 μm long. Both treated and untreated CNTs have high aspect ratios (in the order of 100) and were dispersed in an epoxy resin (Araldite LY556, Huntsman, Salt Lake City, UT, USA). A masterbatch sample of 0.3% was first prepared using a high-shear homogeniser (Silverson L4R). Huang et al. (2006) pointed out that a mixing time of at least several hours was required to establish stable rheology and uniformity at the micron-level. A mixing time of 5 h was

used in this study, and lower-concentration samples were prepared by diluting the masterbatch sample.

Experimental setup

Figure 1 shows the schematic diagram of the filament thinning experiment. Similar filament stretching devices have been previously reported by others (see, for example, Bazilevsky et al. 1990; Matta and Tytus 1990) and have been applied to study extensional rheology of various types of liquids (see, for example, Liang and Mackley 1994; Anna et al. 2001b). Detailed discussions on filament stretching rheometry can be found elsewhere (McKinley 2000; McKinley and Tripathi 2000; McKinley and Sridhar 2002). The filament stretching reported in this paper was achieved using a modification of a Cambridge Multipass Rheometer (MPR) (Tuladhar and Mackley 2008). The MPR is a double-piston device, and in the filament stretching configuration, the barrel and centre section of the rheometer are not used. The servo hydraulically driven pistons can move the top and bottom endplates and, unlike other filament stretching units, the endplates can move in vertically opposite directions, leaving the centre of the filament in the same position throughout the test. A liquid sample was first loaded between the cylindrical endplates with a diameter of 1.2 mm and an initial separation (L_0) of $600 \pm 10 \mu\text{m}$, forming a liquid bridge. Simulations by others (Harlen 1996; Yao et al. 2000) suggested that the initial shape and aspect ratios of the liquid bridge can greatly affect the evaluation of extensional viscosity and the characteristic relaxation time for viscoelastic fluids; an

Fig. 1 Schematic diagram of the filament thinning experiment showing top and bottom cylindrical endplates and fluid contained between the endplates for **a** the initial condition ($t=0$) and **b** an arbitrary later time t



initial aspect ratio ($\Lambda_0 = L_0/R_0$) of 1 was therefore used following the suggestion by Anna and McKinley (1999). Both endplates were moved apart (at $t=0$) by a known distance (d) and at a constant rate (L). Once the endplates had stopped, the filament thinning process was then followed using a high-speed camera (Kodak Motion Corder Analyser Model SR Ultra-C) with a frame rate of 500 frames per second and a resolution of 512×240 pixels, and the filament diameter was calculated from the digital images where 1 pixel = $5.6 \mu\text{m}$. In terms of shear rheology, apparent viscosities of the epoxy resin and the CNT suspensions were measured at 25°C using the ARES strain-controlled rheometer (TA Instrument, New Castle, DE, USA) with 50-mm parallel plates (Fig. 2). Optical microstructure was followed using the Cambridge Shear System (CSS450, Linkam Scientific Instruments, Surrey, UK) with an optical depth of $130 \mu\text{m}$.

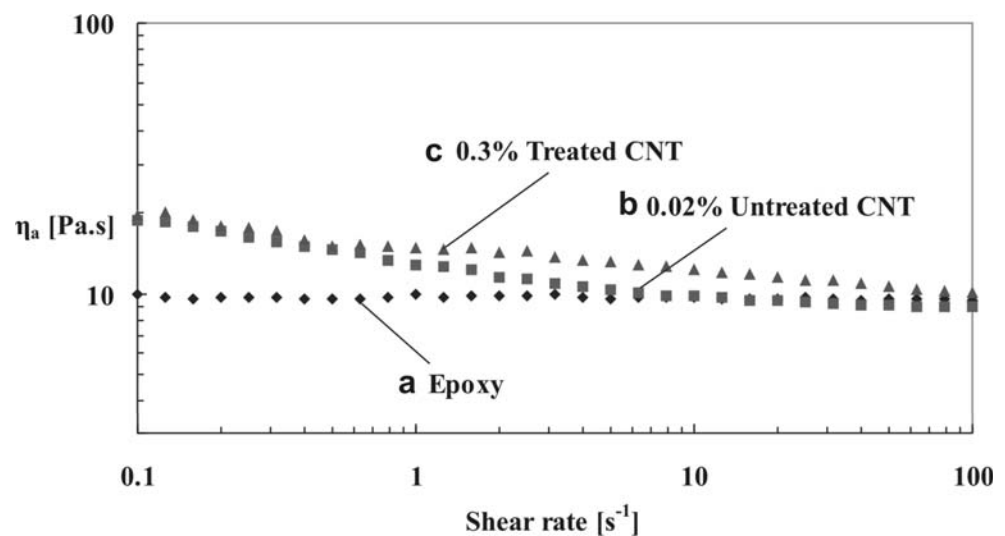
Results and discussion

Filament profile and breakup time

In terms of shear rheology, untreated CNT suspensions generally exhibit a larger shear viscosity enhancement effect than treated CNT suspensions with the same weight loading (Xu et al. 2005; Ma et al. 2007a). To enable direct comparison of the extensional rheology between treated and untreated CNT suspensions, zero-shear-rate viscosities of the two suspensions were matched. This means that the concentration of the untreated CNT suspension (0.02%) was much lower than that of the treated suspension (0.3%). At these respective concentrations, zero-shear-rate viscosity was 20 Pa s. Figure 3 compares profiles for the filaments formed by epoxy, 0.02% untreated and 0.3% treated CNT

suspensions. It was experimentally observed that both treated CNT suspension and epoxy formed a smoothly necked filament (Fig. 3a, c), whereas, for the untreated CNT suspension, heterogeneities were observed and the filament did not break at the mid-point (Fig. 3b). Such difference was also observed for other concentrations, so this could therefore provide a qualitative means to differentiate between treated and untreated CNT samples. Both the heterogeneity of the necking filament and asymmetric breakup of the filament for untreated CNT suspensions, however, prevent appropriate evaluation of extensional viscosity from the filament thinning process. Figure 4a–c show the filament profile before breakage, and corresponding optical micrographs are shown in Fig. 4d–f. The heterogeneities as observed in Fig. 4b for the untreated CNT suspension are consistent with the CNT aggregates as observed in Fig. 4e using optical microscopy, therefore suggesting that the non-uniformity along the filament length is due to the presence of optical microstructure. The rheological behaviour of untreated CNT suspensions is complicated both in terms of its capillary thinning response and steady shear rheology. Steady shear experiments showed that untreated CNT suspensions exhibited a very significant shear-thinning characteristic—addition of 0.1% of CNT resulted in an order-of-magnitude increase in the zero-shear-rate viscosity, and the suspension viscosity shear-thinned to the matrix viscosity at high shear rates [as shown in Fig. 5; see also Rahatekar et al. (2006)]. The shear-thinning response of untreated CNT suspensions was subsequently modelled, and modelling results suggested that CNT aggregation played a very important role in their complex rheological responses. This finding forms an important part of ongoing research, and detailed rheological modelling of CNT aggregate suspensions will be reported in a future paper.

Fig. 2 Apparent steady shear viscosity (η_a) of **a** epoxy, **b** 0.02% untreated CNT and **c** 0.3% treated CNT suspensions. Temperature = 25°C



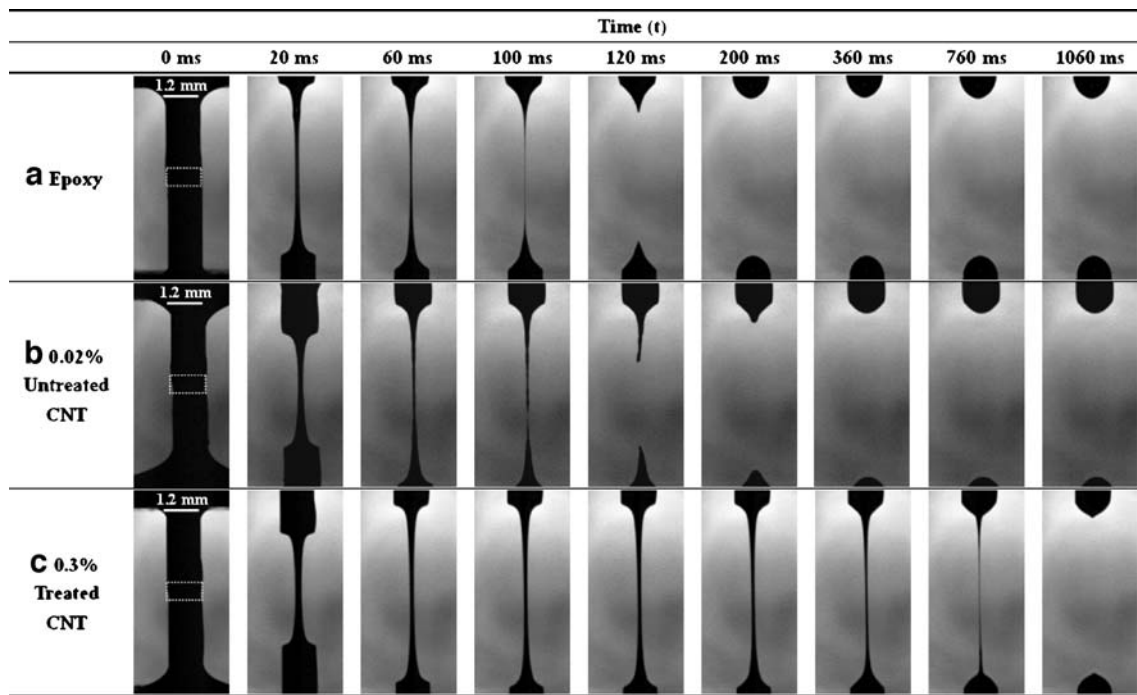


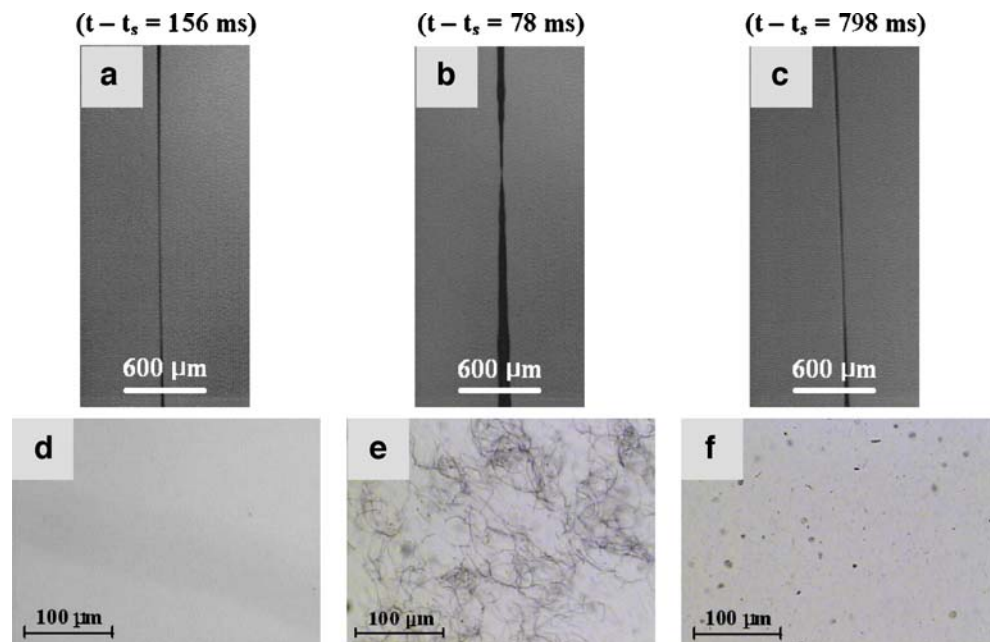
Fig. 3 Sequence of images showing the extensional deformation for the filaments of **a** epoxy, **b** 0.02% untreated CNT suspension and **c** 0.3% treated CNT suspension. Stretching rate=100 mm/s; endplate

displacements=3 mm from starting positions. The initial location of liquid sample at $t=0$ ms highlighted using *dotted lines*

Filament breakup times for the base epoxy, treated and untreated CNT suspensions are presented in Fig. 6, and each of them was computed from four separate experimental runs. A filament formed by the 0.3% treated CNT suspension broke at a time significantly longer than those formed by the epoxy resin and the 0.02% untreated CNT suspension. In the context of rigid rod suspension model-

ing, an increase in the breakup time can be explained in terms of the rods orientating in the stretching direction, causing an increase in the extensional viscosity and slower filament diameter decay (see, for example, Zirnsak et al. 1994; Petrie 1999). The untreated CNT filament thinned in a non-homogeneous manner, creating instability and resulting in the early breakup of the filament.

Fig. 4 **a–c** The filament profile before breakage for **a** epoxy, **b** 0.02% untreated CNT and **c** 0.3% treated CNT. **d–e** Corresponding optical micrographs captured using the Cambridge Shear System (CSS450, Linkam Scientific Instruments) with an optical depth of 130 μm



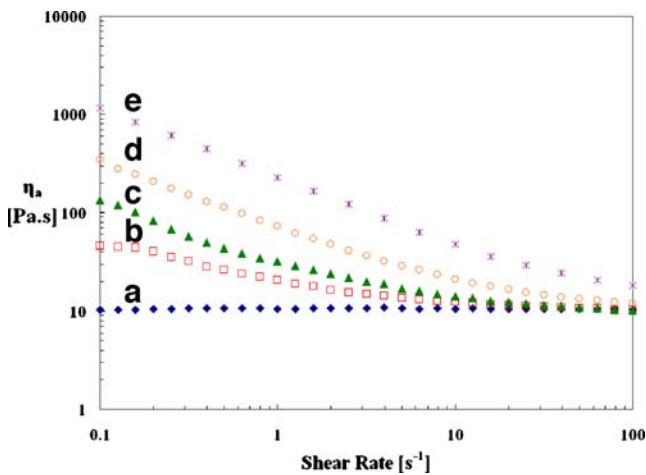


Fig. 5 Apparent steady shear viscosity (η_a) of **a** epoxy, **b** 0.05%, **c** 0.1%, **d** 0.25% and **e** 0.5% untreated CNT suspensions, showing significant viscosity enhancement at relatively low CNT concentration levels

Calculation of extensional viscosity

Figure 7 shows the detailed time evolution of minimum filament diameter (D_{min}) for epoxy, 0.02% untreated CNT and 0.3% treated CNT suspensions. Experimentally, it was observed that, for the epoxy resin and the treated CNT suspension, the minimum filament diameter occurred at the mid-point position (i.e. $D_{min}=D_{mid}$), whereas the filament breakup point for an untreated CNT suspension varied for different experimental runs. In all three cases, a linear decrease in the minimum filament diameter was observed, as shown in the inset figure of Fig. 7, indicating the liquid samples behaved essentially in a Newtonian way during the filament thinning process. The extensional viscosity (η_E) for smoothly necked and axially symmetric filaments can be calculated using the following equation (see, for example, McKinley and Tripathi 2000):

$$\eta_E(t) = (2X - 1) \frac{\sigma}{\left(-\frac{dD_{mid}(t)}{dt}\right)} \tag{1}$$

where D_{mid} is the mid-point filament diameter, σ is the surface tension of the fluid ($\sigma=0.047$ Nm for the epoxy resin), and X is a dimensionless number which was suggested to be 0.7127 for a viscous filament having a smoothly necked profile (Papageorgiou 1995). Detailed derivation and assumptions for Eq. 1 were reported by McKinley and Tripathi (2000). Based on both simulation results and experimental data, they concluded that a proper evaluation of η_E necessitates the use of an X factor, which takes into account the fact that the shape of a filament deviates from a uniform cylindrical thread. In this study, the shear viscosity (η) of the epoxy resin was independently measured to be 10 Pa s using an ARES strain-controlled

rheometer. For a simple Newtonian fluid or the epoxy resin used (Fig. 2), the theoretical value for η_E should be three times the value of η_s , which corresponds to a value of 30 Pa s. From the filament thinning experiment carried out in this paper, the extensional viscosity for the pure epoxy resin was determined to be 27.3 Pa s, further supporting the use of Eq. 1 and an X factor of 0.7127. In general, Eq. 1 allows for the calculation of extensional viscosity based on the slope of a diameter thinning profile after initial stretching. For the 0.3% treated CNT suspension, the extensional viscosity was calculated to be 164.6 Pa s based on four separate experimental runs. Given a zero-shear-rate viscosity of 20 Pa s, this corresponds to a Trouton ratio of 8.2, which is larger than that for a simple Newtonian fluid, implying that the extensional viscosity was enhanced due to the presence of treated CNTs. In the case of the 0.02% untreated CNT suspension, direct application of Eq. 1 would give an extensional viscosity value of 48.2 Pa s, corresponding to a Trouton ratio of 2.4. This calculated value, however, is believed to be unreliable because the analysis of Eq. 1 assumes uniform curvature throughout the filament.

The Bond number (Bo), as defined in Eq. 2, can be computed to assess the relative importance of gravitational force on the filament thinning process (Anna and McKinley 2001a).

$$Bo = \frac{\rho g D_o^2}{4\sigma} \approx 0.098 \tag{2}$$

The Bo number was calculated to be considerably small ($\ll 1$), confirming that gravitation sagging is unimportant compared with the capillary forces.

As pointed out in earlier work by Liang and Mackley (1994), during filament thinning, the strain rate increases as the filament diameter decreases, and the maximum Hencky strain that can be picked up depends on the resolution of

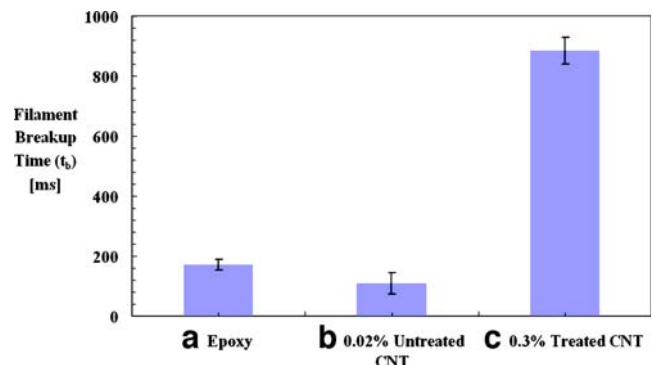
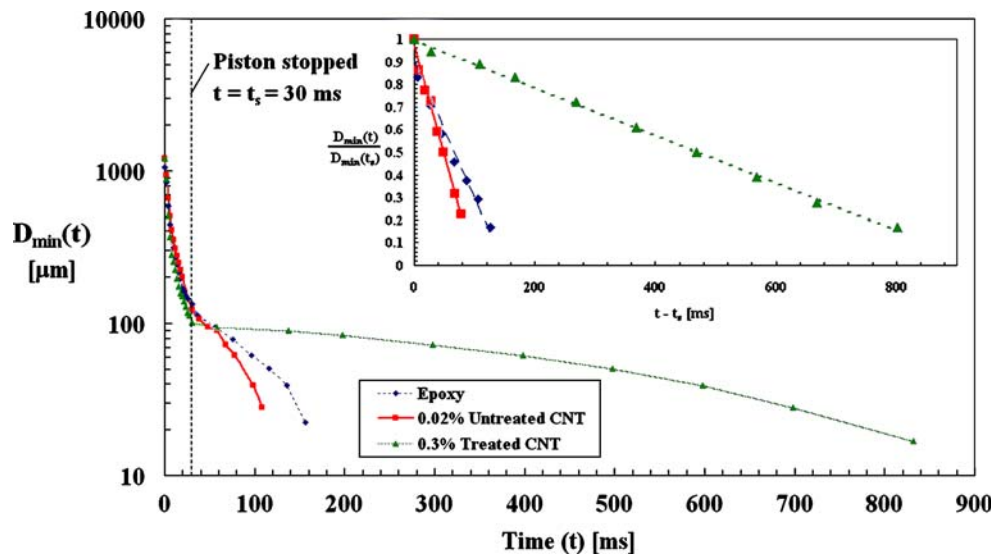


Fig. 6 Filament breakup time (t_b) for **a** epoxy, **b** 0.02% untreated CNT suspension and **c** 0.3% treated CNT suspension. Stretching rate= 100 mm/s and endplate displacements=3 mm from starting positions

Fig. 7 Time evolution of the minimum filament diameter (D_{\min}) for a stretching rate of 100 mm/s and endplate displacements of 3 mm from starting positions. The inset figure shows the normalised filament diameter [$D_{\min}(t)/D_{\min}(t_s)$] as a function of $(t-t_s)$, where t_s is the time at which the endplates stopped. [In the case of epoxy and treated CNT suspensions, D_{\min} occurred at the mid-point of the filament (i.e. $D_{\min}=D_{\text{mid}}$), and this is not necessarily true for the untreated CNT suspension where the filament is asymmetric.]



digital images for the filament, which is given as (Anna and McKinley 2001a):

$$\varepsilon_{\max} = 2 \ln \left(\frac{1.2\text{mm}}{5.6\mu\text{m}} \right) = 10.7 \quad (3)$$

Interestingly, although the addition of treated CNT increased the filament breakup time and the magnitude of η_E , no experimental evidence of strain-hardening during the filament thinning process was observed. Given the large strain input used in this study ($L/L_0=5$), it is assumed that this high level of initial stretch has aligned most of the treated CNTs and additional filament thinning does not result in further alignment of the CNTs. A similar observation was reported, for example, in glass-fibre suspensions (Weinberger and Goddard 1974). The degree

of CNT orientation is estimated in the mechanical modelling section using a simple orientation model.

The effect of initial stretching rate

The filament thinning experiments were repeated for the 0.3% treated CNT suspension using different initial stretching rates (L). However, it was found that the filament thinning analysis could only be performed within a limited range of stretching rates, as shown in Fig. 8. At low piston speeds, below 5 mm/s, the filament broke during the stretching period. At piston speeds above 150 mm/s, there was a damped oscillation for the current setup after the cessation of piston movement, causing the filament to buckle (Fig. 8). This limited measurements to the range of 5–150 mm/s.

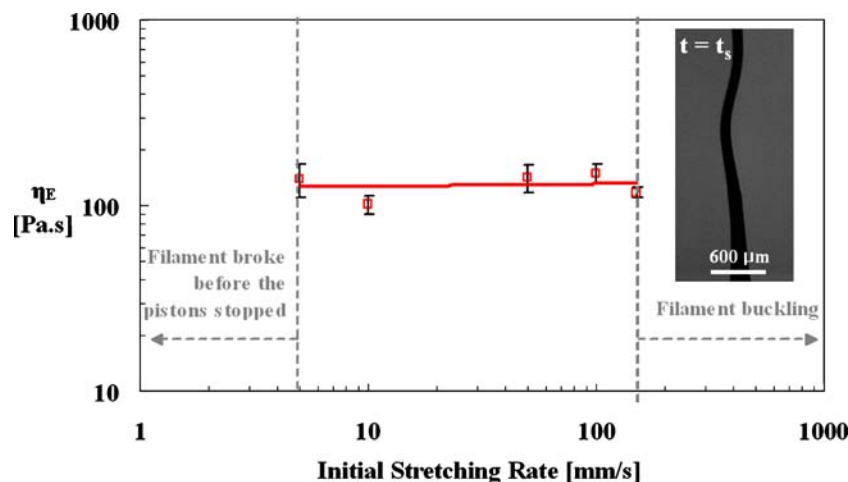


Fig. 8 Extensional viscosity (η_E) derived from Eq. 1 for 0.3% treated CNT suspension as a function of the initial stretching rate. Each open square represents the average value from four separate runs of

experiment. Endplate displacements=3 mm from starting positions. The picture shows filament buckling occurred at a stretching rate of 200 mm/s

Fig. 9 Filament breakup time (t_b) as a function of CNT concentration by weight (C). The breakup time is with reference to the time at which the endplates stopped (t_s). Error bars indicate the standard deviation of four separate runs of experiment. The dotted line represents the best exponential fit where $t_b = 199 e^{1214 C}$ and the solid line represents the best linear fit where $t_b = 188847 C + 301$

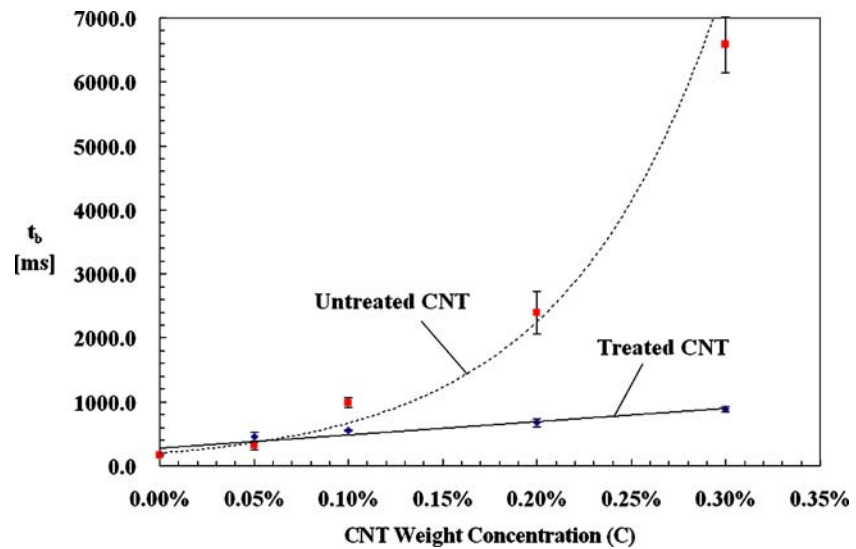


Figure 8 shows that, within the specified range, the extensional viscosity measured by the subsequent filament thinning was essentially independent of the initial stretching rate, again supporting the belief that full orientation is reached during stretching and the orientation level does not further change during the filament thinning process.

The effect of concentration

Filament breakup times for both treated and untreated CNT suspension filaments at different concentrations are shown in Fig. 9. Given the same weight concentration, untreated CNT filaments typically broke at a longer time compared with the treated CNT filaments. Filament breakup time depends on the balance between viscous and capillary forces (Anna and McKinley 2001a), and for the same concentration, larger shear viscosity enhancement effects were generally observed for untreated CNT suspensions (Xu et al. 2005; Ma et al. 2007a). Longer filament breakup times for untreated CNT suspensions can therefore simply be explained in terms of the suspension’s base viscosity. It

was also observed that filament breakup time for untreated CNT suspensions increased roughly as an exponential function of CNT concentration, whereas the breakup time for treated suspensions increased linearly.

The time evolution of filament diameter for different concentrations of treated CNT suspensions was followed and is shown in Fig. 10, where the filament diameter of the treated CNT suspensions decreased linearly as a function of time. The extensional viscosity for treated CNT suspensions was calculated using Eq. 1, and the numerical values for η_E and the Trouton ratio are given in Table 1. The results show that, for treated CNT suspensions, the Trouton ratio is greater than 3, indicating an enhancement extensional viscosity due to the CNTs.

Early work by Batchelor (1971) estimated the values of η_E for a semi-dilute suspension of fibres where the fibres are fully aligned; Batchelor proposed the following expression:

$$\eta_E = \eta_s \left(3 + \frac{4\phi r^2}{3 \ln(\pi/\phi)} \right) \tag{4}$$

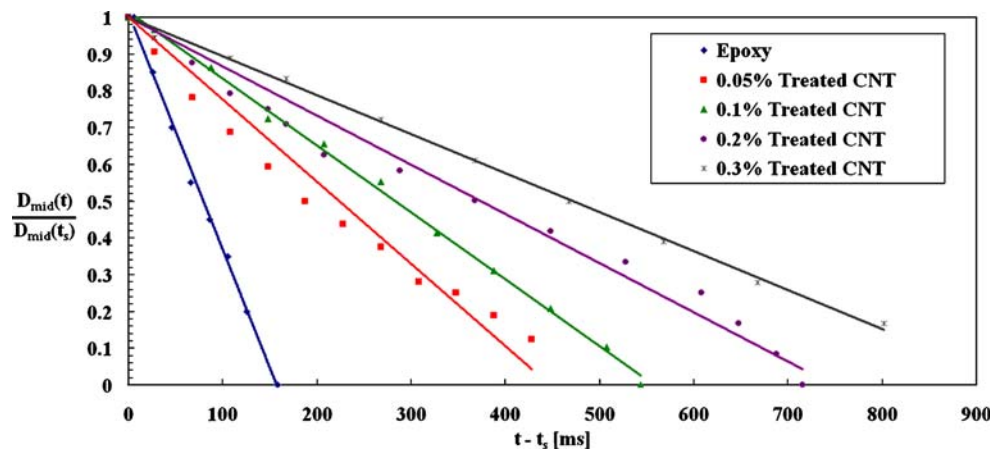
where η_s is the suspending medium viscosity, r is the aspect ratio and ϕ is the volume fraction.

Table 1 Numerical values of extensional viscosity (η_E) and filament breakup time (t_b) for treated CNT suspensions

Weight percent of treated CNTs	Volume percent of treated CNTs	t_b (ms)	η_E (Pa s) (with $X=0.7127$)	Trouton ratio ($=\eta_E/\eta_{S0}$)
0%	0%	171.3	27.4	2.7
0.05%	0.04%	458.0	61.0	5.1
0.10%	0.08%	554.7	66.5	5.1
0.20%	0.17%	674.7	103.8	6.2
0.30%	0.25%	884.0	164.6	8.2

Values shown are averaged from four separate runs of experiment. Volume percents of treated CNTs were calculated using a density of 1,300 kg/m³ for treated CNTs and a density of 1,090 kg/m³ for the epoxy resin. CNT suspensions are shear-thinning and the Trouton ratio is defined with respect to the low shear viscosity (η_{S0})

Fig. 10 Time evolution of normalised filament diameter as a function of $(t-t_s)$, where t_s is the time at which the endplates stopped. Stretching rate=100 mm/s. Endplate displacements=3 mm from initial positions



Shaqfeh and Fredricksen (1990) ignored Brownian motion and proposed the following expression for semi-dilute suspensions involving cylindrical and aligned fibres:

$$\eta_E = \eta_s \left(3 + \frac{4\phi r^2}{3[\ln(1/\phi) + \ln(\ln(1/\phi)) + 0.1585]} \right) \quad (5)$$

Based on filament thinning experiment and Eq. 1, experimental values of η_E are presented as a function of volume fraction in Fig. 11. The figure also shows the predictions by Batchelor (1971) and Shaqfeh and Fredricksen (1990), and the best fit to experimental data was observed with an aspect ratio of 180 (Fig. 11). This result was consistent with the aspect ratio of treated CNT bundles estimated from AFM studies.

The level of CNT orientation within treated CNT suspensions

In the case of short fibre suspensions, the following constitutive equation is applicable to relate the total stress (σ) with fibre orientation (see, for example, Batchelor 1970; Hinch and Leal 1975, 1976):

$$\sigma = -p\mathbf{I} + 2\eta_s\mathbf{D} + 2\eta_s N_p \mathbf{a}_4 : \mathbf{D} \quad (6)$$

where p is the hydrostatic pressure, \mathbf{I} is the identity matrix, η_s is the viscosity of the suspending medium (=10 Pa s), N_p is a parameter that depends on the fibre concentration and aspect ratio, \mathbf{a}_4 is the fourth-order orientation tensor and \mathbf{D} is the strain rate tensor (symmetric part of the velocity gradient tensor) describing the fluid kinematics.

The orientation tensor involved in Eq. 6 can be computed from the fibre orientation distribution $\psi(x, t, \rho)$, which gives the fraction of fibres oriented in the direction ρ at point x in space and at time t . The evolution of the fibre orientation distribution is governed by the Fokker–Planck equation (see, for example, Leal and Hinch

1973), giving the following expressions for the fourth-order (\mathbf{a}_4) and second-order (\mathbf{a}_2) orientation tensors:

$$\mathbf{a}_4 = \int \rho \otimes \rho \otimes \rho \otimes \rho \psi(\rho) d\rho \quad (7)$$

$$\mathbf{a}_2 = \int \rho \otimes \rho \psi(\rho) d\rho \quad (8)$$

with $Tr(\mathbf{a}_2)=1$.

One important underlying assumption in the simple orientation model is that CNT aggregation in treated CNT suspensions is negligible and that the suspension rheology is essentially controlled by CNT orientation. The large magnitude of strain input ($L/L_0=5$) justifies the use of

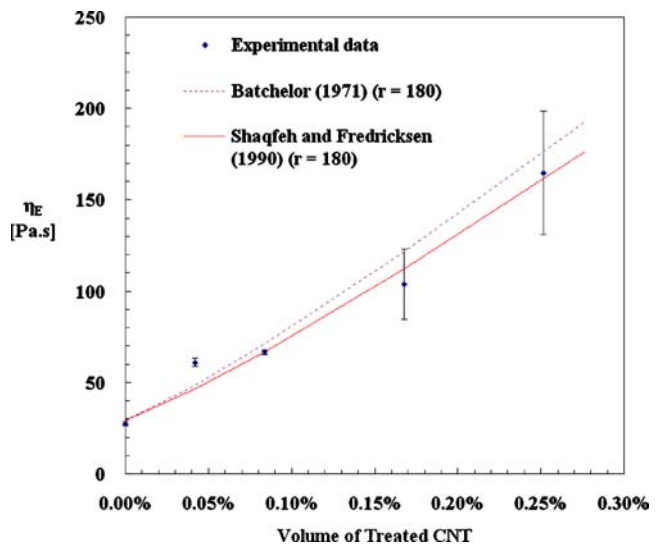
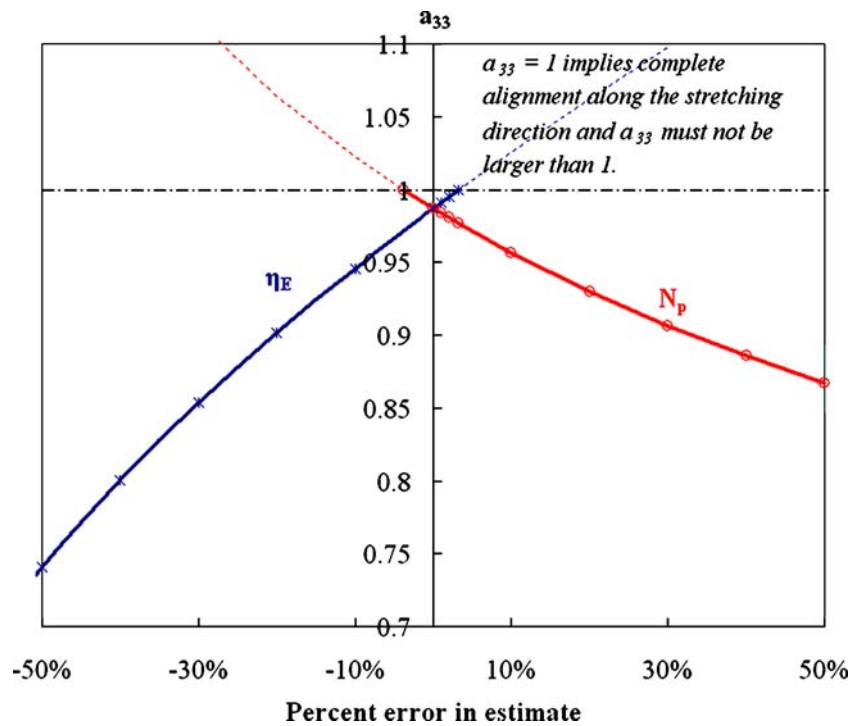


Fig. 11 Extensional viscosity (η_E) as a function of volume fraction. Experimental data were represented by diamonds. The dotted line shows the Batchelor (1971) prediction and the solid line shows the Shaqfeh and Fredricksen (1990) prediction for semi-dilute suspensions involving fibres with a best-fit aspect ratio (r) of 180

Fig. 12 Sensitivity analysis of the level of CNT orientation (a_{33}) for the 0.3% treated CNT suspension as a function of possible errors in determining the extensional viscosity based on capillary thinning experiments and estimating rheological parameter N_p from fitting a Fokker–Planck based simple orientation model to the experimental steady shear data



Eq. 6, which assumes that the contribution of Brownian motion and rotary diffusion of CNTs to the total stress of the system is negligible. Treated CNTs were modelled as rigid rods that can orient and align with the flow, and if the parameter N_p is known, the level of orientation can be estimated using Eq. 6. The numerical values of N_p for two different concentrations were identified by fitting a Fokker–Planck-based simple orientation model to steady shear rheological data (Chinesta, private communication). N_p was determined to be 7 for a 0.3% CNT suspension and $N_p=4$ for a 0.2% CNT suspension. The detailed procedure for obtaining N_p will be reported in a future paper (Ma et al. 2007b). Equation 6 was further applied to quantify the level of CNT orientation after initial stretching.

A quadratic closure approximation can be applied to the last term on the right-hand side of Eq. 6 (Advani and Tucker 1990), which gives:

$$\mathbf{a}_4 : \mathbf{D} \approx (\mathbf{a}_2 : \mathbf{D})\mathbf{a}_2 = Tr(\mathbf{a}_2 \cdot \mathbf{D})\mathbf{a}_2 \tag{9}$$

where $\mathbf{a}_2 = \begin{pmatrix} a & 0 & 0 \\ 0 & a & 0 \\ 0 & 0 & 1-2a \end{pmatrix}$, $\mathbf{D} = \begin{pmatrix} -0.5\dot{\epsilon} & 0 & 0 \\ 0 & -0.5\dot{\epsilon} & 0 \\ 0 & 0 & \dot{\epsilon} \end{pmatrix}$ for

the uniaxial elongation of an incompressible fluid and $\dot{\epsilon}$ is the strain-rate in the z direction (as shown in Fig. 1). The closure approximation given in Eq. 9 becomes an exact expression (i.e. $\mathbf{a}_4 = \mathbf{a}_2 \otimes \mathbf{a}_2$) when all CNTs are completely aligned.

Because $Tr(\mathbf{a}_2 \cdot \mathbf{D}) = -0.5a\dot{\epsilon} - 0.5a\dot{\epsilon} + (1-2a)\dot{\epsilon} = (1-3a)\dot{\epsilon}$, Eq. 9 can therefore be further written as:

$$\begin{aligned} \mathbf{a}_4 : \mathbf{D} &= Tr(\mathbf{a}_2 \cdot \mathbf{D})\mathbf{a}_2 \\ &= \begin{pmatrix} a(1-3a)\dot{\epsilon} & 0 & 0 \\ 0 & a(1-3a)\dot{\epsilon} & 0 \\ 0 & 0 & (1-2a)(1-3a)\dot{\epsilon} \end{pmatrix} \end{aligned} \tag{10}$$

Substituting Eq. 10 into Eq. 6 gives:

$$\begin{cases} \sigma_{xx} = -p - \eta\dot{\epsilon} + 2\eta N_p c_1 \dot{\epsilon} \\ \sigma_{yy} = -p - \eta\dot{\epsilon} + 2\eta N_p c_2 \dot{\epsilon} \\ \sigma_{zz} = -p + 2\eta\dot{\epsilon} + 2\eta N_p c_3 \dot{\epsilon} \end{cases} \text{ where } \begin{cases} c_1 = a(1-3a) \\ c_2 = a(1-3a) \\ c_3 = (1-2a)(1-3a) \end{cases} \tag{11}$$

$$\eta_E = \frac{\sigma_{zz} - \sigma_{xx}}{\dot{\epsilon}} = 3\eta + 2\eta N_p (c_3 - c_1) \tag{12}$$

Based on Eq. 1, η_E was experimentally determined to be 164.6 Pa s for the 0.3% treated CNT suspension, and the value of a can be obtained by solving Eq. 12, which gives:

$$\mathbf{a}_2 = \begin{pmatrix} 0.0065 & 0 & 0 \\ 0 & 0.0065 & 0 \\ 0 & 0 & 0.99 \end{pmatrix} \tag{13}$$

The resulted second-order-orientation tensor (\mathbf{a}_2) indicated that about 99% of the treated CNTs were oriented in the z-direction after initial stretching. Similarly, it was estimated that about 97% of the CNTs was aligned towards the stretching direction in the case of 0.2% treated CNT suspension. High degree of CNT alignment justifies the use of predictions in Eqs. 4 and 5 and a quadratic closure relationship in Eq. 9, which is appropriate for systems in which the fibres are highly aligned. Finally, sensitivity analysis of a_{33} on the experimentally determined η_E and N_p was carried out for the 0.3% treated CNT suspension, and the result is shown in Fig. 12. It is clear from the figure that calculation of the level of CNT orientation is sensitive to both the values of the experimentally determined extensional viscosity and the rheological parameter N_p . In Fig. 11, the error bar for the 0.3% treated CNT suspension represents an experimental error of $\pm 21\%$ in determining the value of η_E . According to Fig. 12, a 21% error in estimating the value of η_E would give a value of a_{33} between 0.9 and 1, therefore suggesting about 90 to 100% of the treated CNTs were aligned in the stretching direction after a strain input of $L/L_0=5$.

Conclusions

An extensional filament stretching protocol has been developed for CNT/epoxy systems, and differences in behaviour between base epoxy, treated and untreated CNTs were observed. The relaxation of epoxy after stretching is consistent with Newtonian behaviour. The treated CNT suspensions also relaxed in an essentially Newtonian way, but with an enhanced extensional viscosity. The magnitude of extensional viscosity enhancement is consistent with the predictions of Batchelor (1971) and Shaqfeh and Fredricksen (1990) for fully aligned CNT rods with an aspect ratio of 180. The implication of this result is that, during initial stretching, CNTs become predominantly aligned in the filament direction, giving an enhanced extensional viscosity. Untreated CNT suspensions behaved in an irregular manner, and filament was not uniform along its length. This resulted in a reduced breakup time for the same initial viscosity, and it was not possible to obtain reliable extensional viscosity data. We attributed the irregular behaviour to the heterogeneous optical microstructure observed for untreated CNT where there is a clear spatial variation in CNT concentration. Because, at present, CNT loadings are low, the presence of the CNT does not appear to have a dramatic effect on extensional rheology. Orientation and state of aggregation, however, are crucial factors for the electrical, optical and thermal properties of CNT suspensions or composites, and consequently, the knowledge of orientation during processing is important.

Acknowledgements We would like to thank Prof. A. H. Windle and the Department of Materials Science and Metallurgy at the University of Cambridge for providing the multi-walled CNTs and Nanocomposites for providing the single-walled CNTs. Anson Ma would also like to thank the Croucher Foundation Scholarship and the Overseas Research Students Awards Scheme (ORSAS) for providing financial support.

References

- Advani SG, Tucker CL III (1990) Closure approximations for three-dimensional structure tensors. *J Rheol* 34:367–386
- Ajayan PM, Stephan O, Colliex C, Trauth D (1994) Aligned carbon nanotube arrays formed by cutting a polymer resin-nanotube composite. *Science* 265:1212–1215
- Anna SL, McKinley GH (1999) Quantifying the stretching and breakup of dilute polymer solutions in two different filament stretching experiments. In: A. I. Ch. E. Annual Meeting, paper 175a, Dallas, 31 October–5 November 1999.
- Anna SL, McKinley GH (2001a) Elasto-capillary thinning and breakup of model elastic liquids. *J Rheol* 45(1):115–138
- Anna SL, McKinley GH, Nguyen DA, Sridhar T, Muller SJ, Huang J, James DF (2001b) An interlaboratory comparison of measurements from filament-stretching rheometers using common test fluids. *J Rheol* 45(1):83–114
- Batchelor GK (1970) The stress system in a suspension of force-free particles. *J Fluid Mech* 41:545–570
- Batchelor GK (1971) The stress generated in a non-dilute suspension of elongated particles by pure straining motion. *J Fluid Mech* 46:813–829
- Bazilevsky AV, Entov VM, Rozhkov AN (1990) Liquid filament microrheometer and some of its applications. In: Oliver DR (ed) Third European Rheology Conference. Elsevier, New York
- Calvert P (1999) Nanotube composites: A recipe for strength. *Nature* 399:210–211
- Davis VA, Ericson LM, Nicholas A, Parra-Vasquez G, Fan H, Wang Y, Prieto V, Longoria JA, Ramesh S, Saini RK, Kittrell C, Billups WE, Wade Adams W, Hauge RH, Smalley RE, Pasquali M (2004) Phase behavior and rheology of SWNTs in superacids. *Macromolecules* 37:154–160
- Dyke CA, Tour JM (2003) Unbundled and highly functionalized carbon nanotubes from aqueous reactions. *Nano Lett* 3(9):1215–1218
- Dyke CA, Tour JM (2004) Overcoming the insolubility of carbon nanotubes through high degrees of sidewall functionalization. *Chem Eur J* 10:812–817
- Harlen OG (1996) Presentation at the Issac Newton Institute Program on The Dynamics of Complex Fluids, Cambridge, England, April 1996
- Hinch EJ, Leal LG (1975) Constitutive equations in suspension mechanics. Part I. *J Fluid Mech* 71:481–495
- Hinch EJ, Leal LG (1976) Constitutive equations in suspension mechanics. Part II. *J Fluid Mech* 76:187–208
- Huang YY, Ahir SV, Terentjev EM (2006) Dispersion rheology of carbon nanotubes in a polymer matrix. *Phys Rev B* 73: 125422-1-9
- Hussain F, Hojjati M, Okamoto M, Gorga RE (2006) Review article: polymer-matrix, nanocomposites, processing, manufacturing, and application: an overview. *J Compos Mater* 40:1511–1575
- Iijima S (1991) Helical microtubules of graphitic carbon. *Nature* 354:56–58
- Jäder J, Willenbacher N, Engström G, Järnström L (2005) The influence of extensional properties on the dewatering of coating colours. *J Pulp Pap Sci* 31:181–187

- Kordás K, Mustonen T, Tóth G, Jantunen H, Lajunen M, Soldano C, Talapatra S, Kar S, Vajtai R, Ajayan PM (2006) Inkjet printing of electrically conductive patterns of Carbon Nanotubes. *Small* 2:1021–1025
- Leal LG, Hinch EJ (1973) Theoretical studies of a suspension of rigid particles affected by Brownian couples. *Rheol Acta* 12: 127–132
- Liang RF, Mackley MR (1994) Rheological characterization of the time and strain dependence for polyisobutylene solutions. *J Non-Newton Fluid Mech* 52:387–405
- Lin-Gibson S, Pathak JA, Grulke EA, Wang H, Hobbie EK (2004) Elastic flow instability in nanotube suspensions. *Phys Rev Lett* 92:048302-1–048302-4
- Ma AWK, Chinesta F, Mackley MR (2007a) The rheology and microstructure of carbon nanotube suspensions. In: 4th Annual European Rheology Conference, Napoli, 12–14 April 2007 (oral presentation)
- Ma AWK, Chinesta F, Mackley MR (2007b) The rheology and modelling of chemically treated Carbon Nanotube suspensions. *J Rheol* (in review)
- Matta JE, Tytus RP (1990) Liquid stretching using a falling cylinder. *J Non-Newton Fluid Mech* 35:215–229
- McKinley GH (2000) In: Binding DM, Hudson NE, Mewis J, Piau J-M, Petrie CJS et al (eds) *Proceedings of the 13th International Congress on Rheology*, vol 1. British Society of Rheology, Cambridge, pp 15–22
- McKinley GH, Sridhar T (2002) Filament-stretching rheometry of complex fluids. *Annu Rev Fluid Mech* 34:375–415
- McKinley GH, Tripathi A (2000) How to extract the Newtonian viscosity from capillary breakup measurements in a filament rheometer. *J Rheol* 44(3):653–670
- Papageorgiou DT (1995) On the breakup of viscous liquid threads. *Phys Fluids* 7:1529–1544
- Petrie CJS (1999) The rheology of fibre suspensions. *J Non-Newton Fluid Mech* 87:369–402
- Pötschke P, Fomes TD, Paul DR (2002) Rheological behavior of multi-walled carbon Nanotube/polycarbonate composites. *Polymer* 43:3247–3255
- Rahatekar SS, Koziol KKK, Butler SA, Elliott JA, Shaffer MSP, Mackley MR, Windle AH (2006) Optical microstructure and viscosity enhancement for an epoxy resin matrix containing multi-wall carbon nanotubes. *J Rheol* 50(5):599–610
- Saito S (1997) Carbon Nanotubes for next-generation electronics devices. *Science* 278:77–78
- Shaqfeh ESG, Fredricksen GH (1990) The hydrodynamic stress in a suspension of rods. *Phys Fluids A* 2:7–24
- Singh C, Shaffer MSP, Windle AH (2003) Production of controlled architectures of aligned carbon nanotubes by an injection chemical vapour deposition method. *Carbon* 41:359–368
- Tans SJ, Verschueren ARM, Dekker C (1998) Room-temperature transistor based on a single carbon nanotube. *Nature* 393: 49–52
- Tuladhar TR, Mackley MR (2008) Filament stretching rheometry and break-up behaviour of low viscosity polymer solutions and inkjet fluids. *J Non-Newton Fluid Mech* 148:97–108
- Weinberger GB, Goddard JD (1974) Extensional flow behaviour of polymer solutions and particle suspensions in spinning motion. *Int J Multiph Flow* 1:465–486
- Xu J, Chatterjee S, Koelling KW, Wang Y, Bechtel SE (2005) Shear and extensional rheology of carbon nanofiber suspensions. *Rheol Acta* 44:537–562
- Yao M, Spiegelberg SH, McKinley GH (2000) Fluid dynamics of weakly strain-hardening fluids in filament stretching devices. *J Non-Newton Fluid Mech* 89:1–43
- Zirnsak MA, Hur DU, Boger DV (1994) Normal stresses in fibre suspensions. *J Non-Newton Fluid Mech* 54:153–193